Applied Physics Letters PERSPECTIVE scitation.org/journal/apl

Perspectives on spintronics with surface acoustic waves

Cite as: Appl. Phys. Lett. **120**, 220502 (2022); doi: 10.1063/5.0093654
Submitted: 29 March 2022 · Accepted: 20 May 2022 ·
Published Online: 3 June 2022

J. Puebla,[1,a)] Y. Hwang,[1,2] S. Maekawa,[1,3,4] and Y. Otani[1,2]

AFFILIATIONS

[1]CEMS, RIKEN, 2-1 Hirosawa, Wako, Saitama 351-0198, Japan
[2]Institute for Solid State Physics, University of Tokyo, 5-1-5 Kashiwanoha, Kashiwa, Chiba 277-8581, Japan
[3]Advanced Science Research Center, Japan Atomic Energy Agency, Tokai 319-1195, Japan
[4]Kavli Institute for Theoretical Sciences, University of Chinese Academy of Sciences, Beijing 100049, People's Republic of China

[a)]**Author to whom correspondence should be addressed:** jorgeluis.pueblanunez@riken.jp

ABSTRACT

Surface acoustic waves (SAWs) are elastic waves propagating on the surface of solids with the amplitude decaying into the solid. The well-established fabrication of compact SAW devices, together with well-defined resonance frequencies, places SAWs as an attractive route to manipulate the magnetization states in spintronics, all of which is made possible by the magnetostriction and magnetoelastic effects. Here, we review the basic characteristics of SAW devices and their interaction out-of-resonance and in-resonance with the magnetization in thin films. We describe our own recent results in this research field and closely related works and provide our perspectives moving forward.

I. INTRODUCTION

The description of the relation between elastic deformation and magnetization dates back to the 19th century. In 1842, the English physicist James Prescott Joule described how changes of magnetic ordering of a material result in mechanical deformation,[1] an effect nowadays known as magnetostriction. The opposite effect, where a magnetic material under mechanical stress or deformation results in change of magnetic susceptibility, is also true and was first described by the Italian Physicist Emilio Villari in 1865,[2] an effect known as the magnetoelastic effect. Early on, magnetostriction and magnetoelasticity found important applications in sensing technology either by monitoring changes of material dimensions under magnetic fields or changes of magnetic fields under mechanical deformation. For many decades, most of the research and development was limited to quasi-static applied strain. However, new possibilities emerged in the 1960s with the development of efficient excitation and detection of surface acoustic waves (SAWs) at microwave frequencies (MHz-GHz) by using interdigital transducers (IDTs) on top of piezoelectric substrates. Soon after, SAW devices were combined with magnetic films to create magnetoelastic microwave components such as isolators and convolvers.[3,4] Interestingly, SAWs coupled to spintronic systems had more to offer. As first described by Kittel in 1958,[5] spin waves (magnons) can be resonantly excited by acoustic waves (phonons) in the GHz frequency range, opening a route to study magnon dynamics under resonant excitation and magnon–phonon interactions.

In this Perspective, we review the research progress of spintronics with SAWs in the last couple of decades with particular emphasis on our own contributions to the field. We focus our discussion on magnetic thin films coupled to SAW devices excited by IDTs on piezoelectric substrates. Nevertheless, we acknowledge that other relevant research has been reported with SAWs excited by ultra-fast lasers[6,7] and bulk acoustic waves coupled to magnetic systems.[8,9] This Perspective is organized as follows: first, we briefly describe the basic characteristics of SAW devices with thin magnetic films; then we divide our discussion between non-resonant and in-resonant coupling of SAWs with magnetic films; and we conclude by giving an outlook for future research directions.

II. BASIC CHARACTERISTICS OF SAW DEVICES WITH MAGNETIC FILMS

Figure 1(a) shows the schematics of the basic structure of a SAW device for spintronic research in the particular case, where magnetic materials are deposited on top of piezoelectric substrates. Note that deposition of piezoelectric materials on top of magnetic layers is also feasible. The SAW device is composed of two IDT ports on top of a piezoelectric substrate with a magnetic layer deposited in between the two IDT ports. When excited by an rf voltage, one of the IDT ports

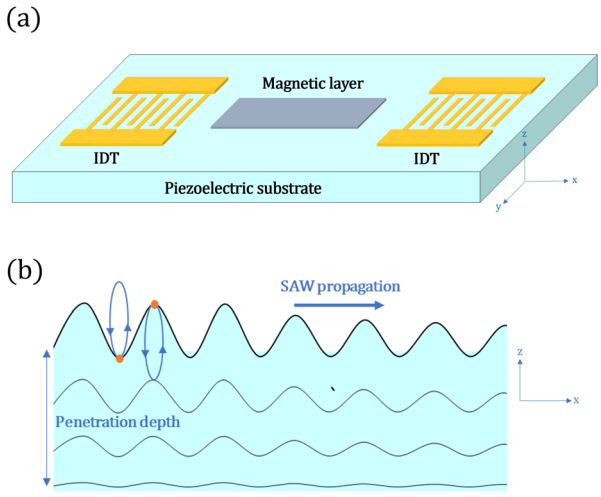

FIG. 1. SAW device with a magnetic layer. (a) Schematic representation of a surface acoustic wave (SAW) device based on interdigital transducers (IDTs) on piezoelectric substrates, coupled to a magnetic layer. (b) Schematic representation of the lattice motion induced by SAWs, SAW propagation, and SAW penetration depth. The SAW penetration depth is of the order of one acoustic wavelength λ_{SAW}.

emits SAWs, which propagate toward the magnetic layer, and the SAWs transmitted through the magnetic layer are detected by the second IDT port, giving information on the absorbed phonon energy and on the dephasing induced by the coupling. In a good approximation, the operating frequency of the SAWs is $f_{SAW} \simeq \upsilon_s/\lambda_{SAW}$, where υ_s is the sound velocity of the piezoelectric substrate and λ_{SAW} is the SAW wavelength defined as $\lambda_{SAW} = 2d$ with d being the period of the transducer finger. Therefore, by selecting the appropriate piezoelectric substrate and IDT design, the desired SAW frequency can be obtained with good precision. As their name suggest, SAWs propagate on the surface of solids with their amplitude decaying inside the bulk with the penetration depth approximately equivalent to one acoustic wavelength λ_{SAW}. Considering that most spintronic research is done in magnetic layers with nanometer thickness, the large majority of spintronic devices are not affected by the limit imposed by the SAW penetration depth. It is important to note that in addition to the strain distribution, SAWs also induce rotation of the lattice, which changes the direction when the SAW propagation direction is reversed. This brief description of SAW devices in spintronics is intended to guide readers unfamiliar with the field as we move forward to the Secs. III, IV and V, where we describe the recent research works, and is not intended to provide a detailed description of the SAW coupling with the magnetization in thin films. If the reader is interested in a deeper description, we refer to recent studies in the topic.[10–12] In the following, we describe the recent works in spintronics with SAWs off and on resonance with the spin wave dispersion in magnetic films.

III. NON-RESONANT COUPLING OF SAWs WITH MAGNETIC FILMS

For non-resonant coupling of SAWs with magnetic films, we interpret the interaction with SAWs without coherent excitation of magnetization precession or spin waves. The non-resonant coupling of SAWs with magnetic films offers routes to assist magnetization switching, domain wall motion, and even creation of nucleation points for magnetic textures such as skyrmions. We describe some of the recent works on these topics.

A. SAW assisted magnetization switching

Figure 2(a) shows a schematic representation of a device similar to the device structure used for strain assisted magnetization switching by Davis *et al.*[13] The device consists of IDTs fabricated on top of a $LiNbO_3$ substrate, and an array of Co wires with 10 nm thickness, 10 μm width and 40 μm long, elongated in the y-axis. Therefore, the hard axis is in the x-axis parallel to the SAW k-wavevector, and the easy axis is along the elongated wire direction. The coordinates here differ from those in the original publication[13] without compromising the concept of the study. Traveling SAWs in the x-axis stretch and compress the Co wires, modulating the energy along the hard axis by $B_1\varepsilon_{xx}$, where B_1 is the magnetoelastic coefficient. If $B_1\varepsilon_{xx}$ is negative, it lowers the energy along the hard axis, facilitating the switching of magnetization from a nominal easy axis to the hard axis. By measuring magneto-optical Kerr effect (MOKE), Davis *et al.*[13] demonstrated that compressive strain induced by SAWs allows magnetization switching in an array of Co wires similar to the schematics in Fig. 2(a) for the magnetoelastic coefficient of Co, $B_1 = 6 \times 10^6$ N/m^2. The fundamental SAW frequency in this study was $f_0 = 91.75$ MHz, away from the frequency region of efficient resonant spin wave excitation.

The demonstration of magnetization switching by SAWs motivates the development of hybrid prototypes of spin transfer torque random access memories based on magnetic tunnel junctions (MTJs). Figure 2(b) shows a schematic of a SAW device with a MTJ structure, which combines SAWs and spin transfer torque (STT) to obtain a highly reliable magnetization switching device. Propagating SAWs produce compressive strain during half of their cycle and tensile strain during the other half cycle. Depending on the sign of the

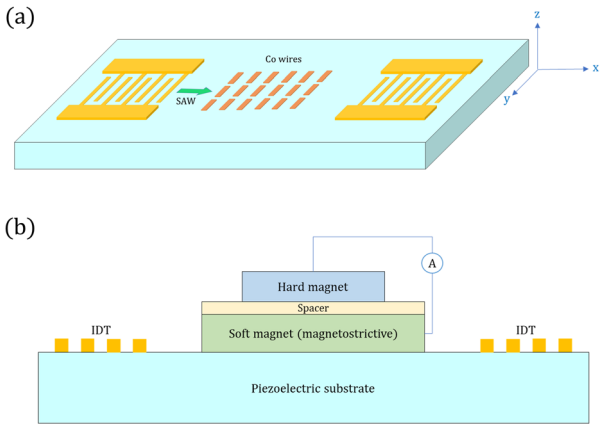

FIG. 2. SAW devices for magnetization switching. (a) Schematic representation of a device similar to the device structure used in a strain assisted magnetization switching study by Davis *et al.*[13] The device consists of IDTs fabricated on top of a $LiNbO_3$ substrate and an array to Co wires with 10 nm thickness, 10 μm width, and 40 μm long, elongated in the y-axis. (b) Schematic of a SAW device with a MTJ structure, which combines SAWs and spin transfer torque (STT) to obtain a highly reliable magnetization switching device based on the numerical study by Biswas *et al.*[14]

magnetoelastic coefficient B_1, one of the SAW half cycles rotates the magnetization toward the hard axis. After the applied SAWs assist the magnetization rotation, a spin polarized current can be passed through a MTJ to selectively switch the magnetization to a desired state. With a similar structure to that in Fig. 2(b), Biswas *et al.*[14] estimated SAW+STT magnetization switching with >99.99% probability at room temperature using a Terfenol-D nanomagnet as the magnetostrictive material and a SAW fundamental frequency $f_0 = 100$ MHz. Moreover, the writing current would also be reduced by a factor of 2.2 with the SAW+STT scheme, making it attractive for energy efficient spintronics.[15]

B. Domain wall motion assisted by SAWs

In 2015, Dean *et al.*[16] reported a study of magnetic domain walls (DWs) interacting with SAWs based on finite-element micromagnetic simulations. In this study, two counter propagating SAWs forming a standing wave interact with a magnetic wire, similar to the schematic in Fig. 3(a). The study by Dean *et al.*[16] describes a magnetic wire with an in-plane magnetic easy axis, a $Fe_{70}Ga_{18}B_{12}$ nanowire. As the starting magnetization, the magnetic domains are head-to-head in a transverse configuration. In each of the micromagnetic simulations, the initial position of the DW is displaced away from the nearest antinode position (AN) of the standing wave. Interestingly, every simulation showed that after a given time t_1, the DW quickly moves to the nearest AN position, as schematically shown in Fig. 3(b). Dean *et al.*[16] used a semi-analytical 1D model to underpin the physical mechanism of the SAW assisted DW motion. When compared with the simulations, the semi-analytical 1D model suggests that the main strain contribution comes from the ε_{xx} component, which is the largest strain component in Rayleigh SAWs. The ε_{xx} strain drives oscillation on both the x-axis DW position and the in-plane magnetization; thus, the DW appears to carry momentum undergoing a ratcheted motion toward the AN position, where ε_{xx} is minimized. Due to this minimized ε_{xx} strain, the DW motion is drastically reduced at the AN positions. To further induce DW motion, Dean *et al.*[16] applied the Doppler effect by increasing the excitation frequency of one IDT port by Δf, effectively creating a traveling standing wave with drift velocity $\nu = \frac{v_{SAW}\Delta f}{f_{SAW}}$, where v_{SAW} is the SAW velocity of the substrate and f_{SAW} is the nominal IDT frequency. The simulation demonstrated that a drifting standing wave carried the DW with an upper limit velocity of 50 m/s, which corresponds to the estimated velocity of the immediate DW motion to the AN positions. The study by Dean *et al.*[16] considered SAW frequency $f_{SAW} = 4.23$ GHz, and at this frequency, resonant excitation of spin waves and magnetization precession is expected, complicating significantly the panorama of their simulation work. Nevertheless, the study accomplished the goal of laying foundations for further research.

Based on the study by Dean *et al.*,[16] Edrington *et al.*[17] performed experiments with a device similar to the schematics in Fig. 3(a); however, in their study, they use a Co/Pt multilayer structure with perpendicular anisotropy on a $LiNbO_3$ substrate with SAW frequency $f_{SAW} = 96.6$ MHz, lessening the probabilities of a more complex scenario with resonant spin wave excitation and coherent magnetic precession. The experiments show an increase in DW velocities of one order of magnitude when the SAW and magnetic field were applied simultaneously than when the magnetic field was applied alone. Another key finding was to observe a significant periodic reduction in the DW velocity at the node (N) and antinode (AN) positions of the standing wave, something suggested only for the AN positions in the previous simulation study.[16] These results relate to a central topic in DW motion, the role of pinning sites and potentials. In a recent study, Adhikari *et al.*[18] examined the use of SAWs as a method for DW depinning in deep pinning sites. Adhikari *et al.*[18] used a variation of the device of Fig. 3(a) with multiple wires aligned parallel to the SAW k-wavevector, connected at both ends by a larger area of DW reservoirs. The material structure is based on Co/Pt multilayers with perpendicular anisotropy on a $LiNbO_3$ substrate with SAW frequency $f_{SAW} = 114.8$ MHz. The wires were irradiated by Argon ion milling, which is known to promote deep pinning sites. The study characterized the depinning probability $P(t)$ of several pinning sites with various strengths while using a combination of pulsed magnetic fields and SAWs. Figure 4 shows the depinning probability $P(t)$ as a function of

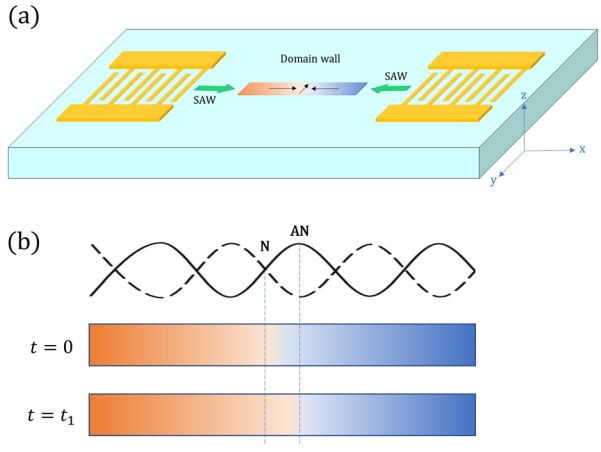

FIG. 3. SAW assisted domain wall motion. (a) Schematic representation of a device similar to that used in the study of domain walls interacting with SAWs by Dean *et al.*[16] (b) Schematic representation of DW motion to the nearest antinode (AN) position in a standing wave formed in the device in (a).

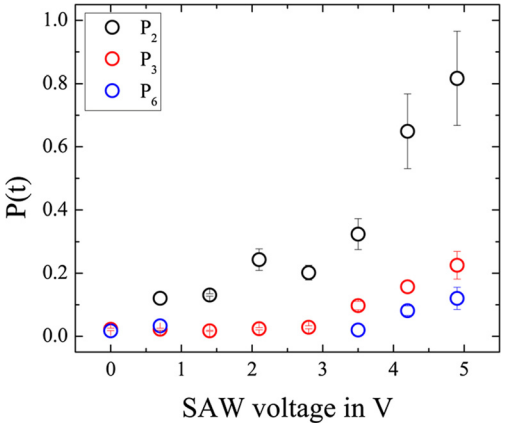

FIG. 4. SAW assisted depinning probability. Depinning probability $P(t)$ as a function of the SAW applied voltage at $f_{SAW} = 114.8$ MHz with a pulsed magnetic field with 5 ms duration and H = 205 Oe. Three representative pinning sites with different strengths are characterized, P_2 (weak), P_3 (intermediate), and P_6 (strong). Figure reproduced from Ref. 18.

the SAW applied voltage with a pulsed magnetic field with 5 ms duration and H = 205 Oe. Three representative pinning sites with different strengths are characterized, P_2 (weak), P_3 (intermediate), and P_6 (strong). All sites' depinning probabilities $P(t)$ are increased with the SAW applied voltage. Analysis showed that the SAWs induce an increase in 4–9 times in depinning probability while assisting pulsed magnetic fields; however, in the absence of magnetic fields, SAWs did not depin even the weakest pinning sites. After ruling out the contribution of heating induced by SAWs, based on a simple model, Adhikari *et al.*[18] suggested that the SAWs increase the depinning probability by magnetoelastic modulation of the energy barriers of the defect sites. Although reasonable agreement exists between the model and the experimental data, the complexity of stress and interference profiles of SAWs, alongside the elastic properties of DWs and their interactions, call for further and more detailed studies.

It is also worth mentioning that Thevenard *et al.*[19] showed a significant reduction in coercivity (up to 60%) of a thin (GaMn)(As,P) layer with out-of-plane magnetization induced by SAW-assisted magnetic domain nucleation with a SAW frequency of f_{SAW} = 549 MHz. Although this study does not contemplate domain wall motion *per se*, SAW-assisted magnetic domain nucleation and lowering of coercivity energy are crucial steps toward efficient SAW driven domain wall motion and generation of on-demand nucleation sites.

C. Skyrmion nucleation assisted by SAWs

Magnetic skyrmions are spin textures with non-trivial topology that appear in magnetic systems with broken spatial inversion symmetry and hold promise as a central element in a new generation of energy efficient nonvolatile memory technology. Naturally, finding methods for energy efficient skyrmion formation is an important motivation. Yokouchi *et al.*[20] demonstrated that SAWs can promote the formation of magnetic skyrmions. In the study, Yokouchi *et al.*[20] used a device similar to that in the schematic of Fig. 1(a) with a Pt/Co/Ir trilayer as the magnetic element on top of a $LiNbO_3$ substrate with SAW resonance frequency f_{SAW} = 230 MHz. Figure 5 shows polar MOKE images of the Pt/Co/Ir trilayer under an external out-of-plane magnetic field of $\mu_0 H = 0.24$ mT before exciting SAWs with rf power P = 251 mW; during SAW excitation (SAW on); and after SAW excitation (SAW off). Right after switching on the SAW excitation, skyrmions appear and are maintained even after the SAW excitation is switched off. The SAW frequency here f_{SAW} = 230 MHz corresponds to a SAW wavelength of $\lambda_{SAW} = 16\,\mu$m. Yokouchi *et al.*[20] observed that the density of created skyrmions with $\lambda_{SAW} = 16\,\mu$m is higher than devices with $\lambda_{SAW} = 8\,\mu$m and 32 μm. The skyrmion average size is 3–6 μm for all three λ_{SAW}, which is smaller than 1/2 of the λ_{SAW} of the primary device. Based on micromagnetic simulations Yokouchi *et al.*[20] demonstrated that the inhomogeneous effective torque induced by the SAWs and thermal fluctuations via the magnetoelastic effect are the main causes of the skyrmion formation. The length scale of the effective torque is in fact smaller than one half wavelength in the simulations in agreement with the largest density of skyrmions with an average size of 3–6 μm for $\lambda_{SAW} = 16\,\mu$m in the experiments. The report by Yokouchi *et al.*[20] opens the possibility of engineering acoustic wave landscapes to generate skyrmions with on-demand positions.

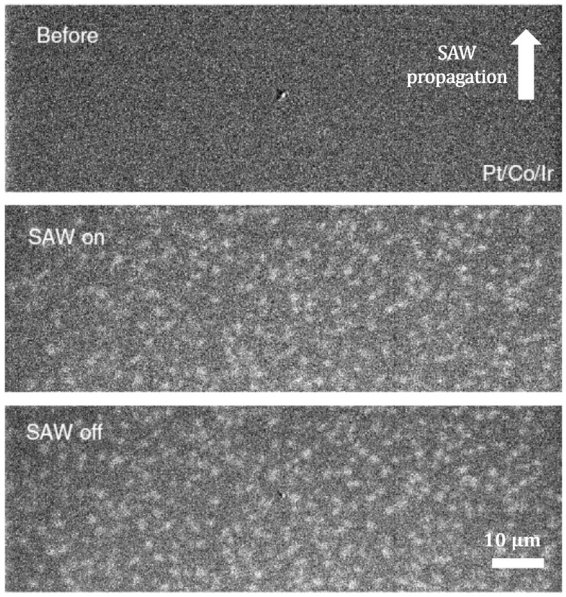

FIG. 5. SAW assisted skyrmion formation. Polar MOKE images of the Pt/Co/Ir trilayer under external out-of-plane magnetic field $\mu H = 0.24$ mT, before exciting SAW with rf power P = 251 mW, during SAW excitation (SAW on), and after SAW excitation (SAW off). Figure reproduced from Ref. 20.

IV. RESONANT COUPLING OF SAWs WITH MAGNETIC FILMS

For resonant coupling of SAWs with magnetic films, we interpret the interaction between SAWs and coherent excitations of magnetization precession or spin waves. We restrict our description to the resonant coupling of SAWs with magnetic films for generation of spin currents via acoustic ferromagnetic resonance and nonreciprocal phenomena. We describe some of the recent works on these topics.

A. Spin current generation via acoustic ferromagnetic resonance

In 1958, Kittel published a theoretical description of the coupling between lattice vibrations (phonons) and spin waves (magnons).[5] It was concluded that microwave phonons in the GHz frequency range would be necessary to resonantly excite magnons. With the development of the IDT method to generate microwave SAWs in the 1960s and their development in the 1970s and 1980s, it became possible to study the resonant excitation of magnons by microwave SAWs. A few decades later, in 2011, Weiler *et al.*[21] reported the successful excitation of ferromagnetic resonance (FMR) by GHz frequency SAWs with a Nickel film deposited on a $LiNbO_3$ substrate. It was observed that the maximum absorption of SAWs driving FMR was obtained at an in-plane magnetic field angle of $\theta = 45°$ from the SAW k-wavevector. Knowing that the magnetization precession produced in FMR can generate spin currents,[22] the same research group followed up with the demonstration of spin current generation excited by SAWs[23] and a more detailed analysis of what is nowadays known as acoustic FMR and acoustic spin pumping.[10,24] Presently, advances in fabrication techniques, such as electron beam lithography, allow to fabricate SAW

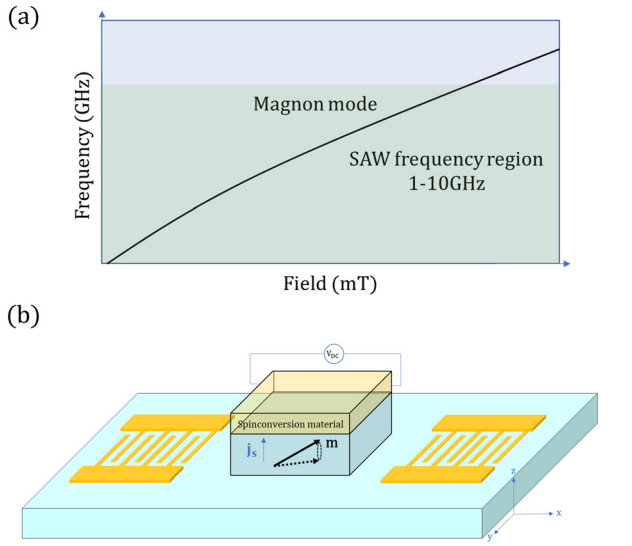

FIG. 6. Acoustic ferromagnetic resonance. (a) Schematic representation of the interaction frequency range of a magnon mode with GHz SAW devices (colored area). (b) Schematic representation of a SAW device for acoustic ferromagnetic resonance and spin pumping.

devices within the frequency range between 1 and 10 GHz and couple them with the magnetic mode dispersion of various materials as schematically shown in Fig. 6(a). Figure 6(b) shows the schematic representation of a SAW device for acoustic ferromagnetic resonance and spin pumping, where the spin-conversion material can be either a spin Hall system[23] or a Rashba interface as we demonstrated in our laboratory.[25]

Note that SAW technology has a longer history than spintronics, such that there are still characteristics and technology advances in SAWs waiting to be exploited in the development of novel spintronic devices. For instance, SAW resonators are a well-developed technology that help one to confine the acoustic waves and increase the Q-factor. With that in mind, in our laboratory, we explored the possibility of enhancement of spin current generation by SAWs confined in between a pair of SAW resonators, forming an acoustic cavity. We fabricated SAW devices with a similar structure to that shown in the schematic representation in Fig. 6(b) with a Ni/Cu/Bi_2O_3 trilayer deposited on top of a $LiNbO_3$ substrate and compared the spin current generation with and without a pair of SAW resonators forming an acoustic cavity.[26] Figure 7 shows the output spin-conversion voltage of the SAW device without Fig. 7(a) and with Fig. 7(b) an acoustic cavity. We demonstrated enhancement of up to three times in spin current generation in the presence of an acoustic cavity. In this study, all distances between IDT ports and SAW reflectors were carefully engineered to be multiples of λ_{SAW}. Further improvements in the Q-factor of the acoustic cavities pave the way to achieve strong magnon–phonon coupling.

B. Nonreciprocity in SAW spintronic devices

The relevance of nonreciprocal phenomena can be captured with the technological success of the electronic diode, which permits flow of

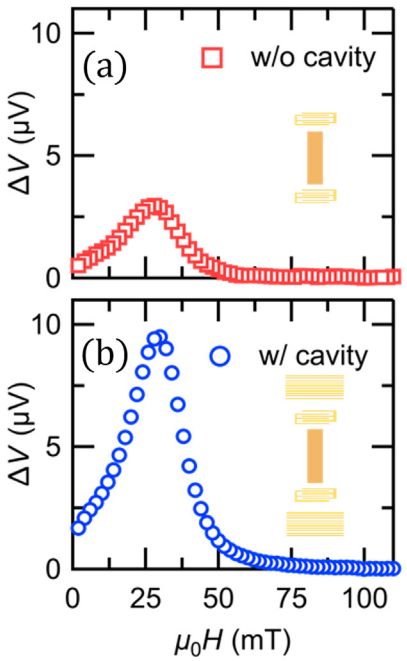

FIG. 7. Enhancement of spin current with SAW resonators. Spinconversion output voltage in a Ni/Cu/Bi_2O_3 trilayer of a SAW device without (a) and with (b) an acoustic cavity.

the electrical current in one direction and blocks it in the opposite direction. Notably, the coupling of SAWs with magnetic thin layers can give rise to nonreciprocal SAW absorption and nonreciprocal resonance frequency. The proposed mechanisms behind the nonreciprocity are various: interference of shear and longitudinal magnetoelastic couplings;[27,28] asymmetric magnetoelastic wave dispersion via Dzyaloshinskii–Moriya interaction (DMI)[29,30] or using ferromagnetic multilayers;[31–33] phonon angular momentum;[34] and magneto-rotation coupling.[35,36] In a brief description, nonreciprocity as a consequence of interference of shear and longitudinal magnetoelastic couplings is applicable to relatively thick layers[37] or thin embedded layers,[38] as the shear strain vanishes for thin layers when the acoustic wavelength is much larger than the layer thickness, $\lambda_{SAW} \gg t_{FM}$. In the case of nonreciprocity via DMI, it is the result of a nonreciprocal spin wave dispersion with origins in intrinsic time reversal symmetry breaking. Regarding nonreciprocity in ferromagnetic multilayers, the interlayer dipolar coupling induces nondegenerate dispersion relations for oppositely traveling spin waves. With the potential for high tunability, nonreciprocity in magneto-rotation coupling has its origins in the chirality of the lattice rotation induced by SAWs.

In our recent related work,[36] we used a device structure similar to that in Fig. 1(a) with a CoFeB layer of 1.6 nm thickness on top of a $LiNbO_3$ substrate. We demonstrated up to 100% nonreciprocal SAW absorption of counter propagating SAWs on CoFeB with an in-plane external magnetic field applied in a small angle (∼184°) with respect to the SAW k-wavevector, as shown in Fig. 8(a). We claimed that the large nonreciprocity is predominantly the result of the magneto-rotation coupling originally proposed by Maekawa and Tachiki more than 45 years ago.[35] A schematic representation of the

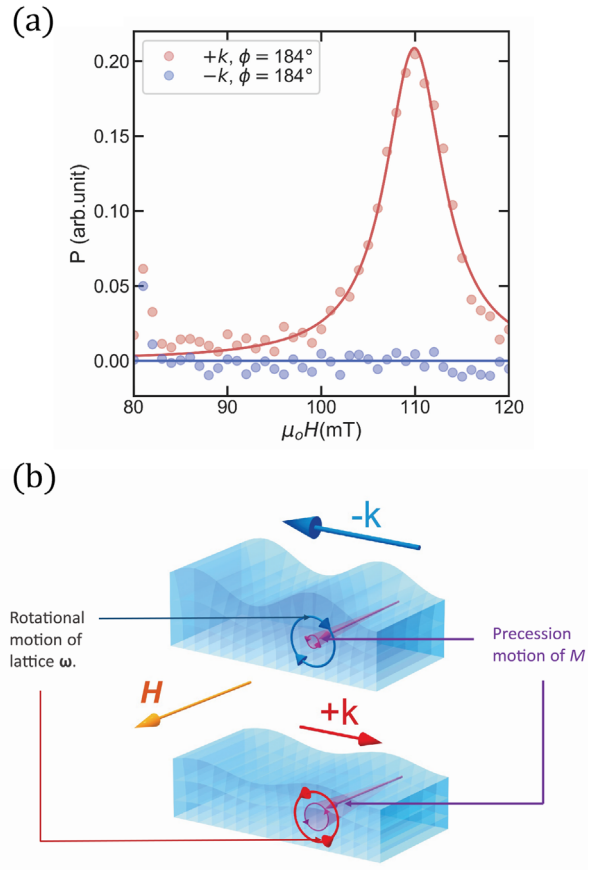

FIG. 8. Nonreciprocity via magneto-rotation coupling. (a) Nonreciprocal SAW power absorption of counter propagating SAWs in a CoFeB thin film (1.6 nm). (b) Schematic representation of the magneto-rotation coupling principle, in which counter propagating SAWs induce opposite lattice chirality. Figures reproduced from Ref. 36.

magneto-rotation coupling is shown in Fig. 8(b). Magneto-rotation coupling has the advantage that it does not require magnetic materials with large magnetoelasticity. Demonstration of this independence from materials with large magnetoelastic effects can be obtained in magnetic alloys with large magnetoelastic tunability such as Permalloy. Here, our description is focused on the nonreciprocity of the SAW absorption magnitude; however, we would like to mention that nonreciprocity of the SAW resonant field absorption also exists and can be used to determine the DMI coefficient in thin films.[30,36]

V. OUTLOOK

Figure 9 shows a roadmap as conceptualized by the authors. We listed the topics described in the present Perspective and proposed four additional research directions to pursue. We first lay out our perspectives on the open challenges in the topics described already here, and then we describe the proposed research directions.

Although significant advances have been achieved in the coupling of SAWs with magnetic DWs, we are still waiting to transport DWs at SAW velocities, which are hindered by the random distribution of pinning sites and complex interference patterns of traveling SAWs. As

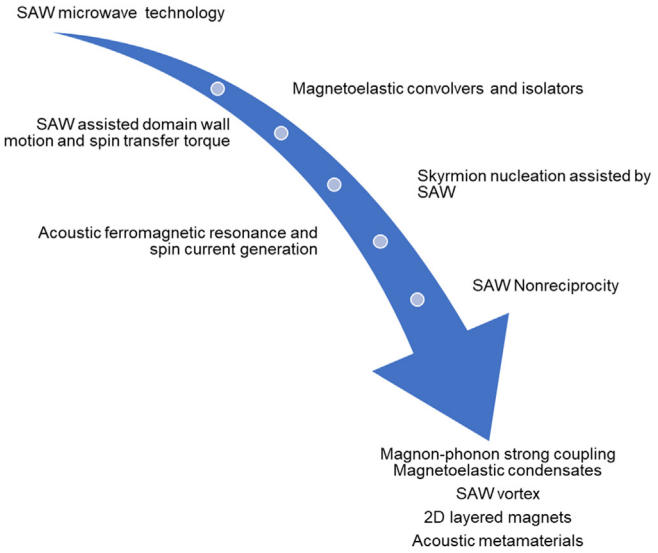

FIG. 9. Roadmap. We schematically show in sequential order the topics discussed in this Perspective and additional four attractive research topics to pursue as intended by the authors.

described before, SAWs can be effective to overcome pinning potentials when combined with DW driving by the charge current or external magnetic fields. Further studies in these directions with more advanced SAW designs to guide the acoustic wave front can give new insight. Regarding the coupling of SAWs with magnetic skyrmions, one attractive option is to make use of the acoustic tweezer developments,[39] and explore the formation and manipulation of skyrmions by designed acoustic potentials. In fact, a recent report showed the experimental observation of skyrmion-like structures made of acoustic waves trapped in a designed hexagonal acoustic metasurface.[40] Regarding the SAW resonant coupling with magnets, we believe that there is still a lot to learn from acoustic ferromagnetic resonance and spin current generation, particularly in the presence of resonant acoustic cavities. In our previous report,[26] we observed a pronounced nonlinear SAW power dependence of the spin current generation. As SAWs are, in principle, linear in power, it is important to clarify the origin of such nonlinearities. The demonstration of nonreciprocity with values up to 100% opens up the route to application developments such as magneto-acoustic rectifiers with the pending confirmation of nonreciprocal effects induced by magneto-rotation coupling in systems with vanishing magnetoelasticity. In the following we comment on the additional proposed research directions.

A. Magnon–phonon strong coupling

Strong coupling physics is a topic of increasing attention since the Nobel Prize winning work on cavity quantum electrodynamics.[41] In spintronics, it opens up the possibility of forming novel hybrid quasiparticles,[42] such as hybrid magnon–phonon quasiparticles. A requirement to achieve strong coupling is to have larger coupling energy g than the energy losses of the involved quasiparticles, such as $g/(\gamma_{ph}, \kappa_m) > 1$, where γ_{ph} are the phonon energy losses and κ_m are the magnon energy losses. This scenario can be accomplished by using

SAW devices with well-engineered acoustic cavities and making use of low damping magnetic materials such as yttrium iron garnet (YIG).

B. Magnetoelastic condensates

Bose–Einstein condensates (BEC) is another fascinating physics phenomena, where high densities of bosonic quasiparticles occupy the same energy state and are de facto indistinguishable, forming a macroscopic state described by quantum statistics. Both phonons and magnons are bosonic quasiparticles and can form BECs, which have been recently experimentally observed in a YIG layer under off-resonant microwave parametric pumping.[43] It would be interesting to obtain magnon–phonon condensates under SAW excitation. As reported by Bozhko *et al.*,[43] different from standard BECs, the magnon–phonon hybridization can stimulate the spontaneous accumulation of magnon–phonon quasiparticles with nonzero group velocity, enabling them to act as information carriers.

C. SAW vortices

The formation of acoustic-mechanical wave vortices is not unusual and has been significantly explored in the past. In aeronautics, for instance, the formation of sound vortices is well documented and typically undesirable. Things get more desirable from a physics perspective, when we conclude that such sound vortex interactions have amplitude and phase components, which can be described by Landau–Lifshitz fluid mechanics and can be measured experimentally. It is an ongoing topic of debate whether or not phonons possess spin and orbital angular momentum. Interestingly, electromagnetism has lots of similarities with acoustics, which gives confidence in the existence of spin and orbital angular momentum in acoustics, similar to those in optics.[44] The experimental demonstration of SAW vortices with well-defined phases coupled to magnetic layers can give insight in the role of orbital angular momentum in magnon–phonon coupling. Inspired by the work done on acoustic tweezers for the manipulation of bioparticles,[45] we show in Fig. 10(a) the schematic representation of a SAW device capable of forming a rotating acoustic vortex with well-defined potential and phase. The distribution of acoustic radiation force forms a potential minimum at the center. Here, the acoustic radiation forces and torques[46] can be used to transfer angular momentum to magnetic layers and perhaps induce magnetic textures with well-defined topological charge.

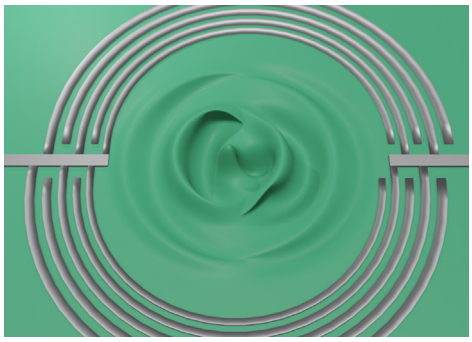

FIG. 10. SAW vortex device. We schematically show a SAW device for the generation of a rotating acoustic vortex given by the shift in the IDT position design. The schematic is inspired by Ref. 45.

D. 2D layered materials

Two-dimensional (2D) layered materials have attracted a tremendous amount of research attention, and one of the latest members of this materials family is the 2D layered magnets. There are already reports suggesting that 2D layered magnets possess significant magnetostriction.[47,48] It is intriguing to explore the coupling of SAWs with 2D layered magnets. In particular, the resonance of 2D layered antiferromagnets lies in the GHz frequency range[49] within the reach of SAW devices, enabling the possibility of the first experimental evidence of SAW resonant coupling with antiferromagnets. Moreover, a well-known and attractive property of layered materials is the strong modifications of their physical properties as they approach the monolayer limit, something that can also be investigated when coupling with SAWs.

E. Acoustic metamaterials

Very recently, we became aware of the fascinating progress in acoustic metamaterials. As is well-known, changes in the landscape traveled by waves affects their propagation and under careful design can determine the travel path *a priori*, as extensively described by Leon Brillouin in his book "*Wave Propagation in Periodic Structures*," originally published in 1946.[50] In more recent years, advances in numerical simulations have revealed more realistic scenarios for artificial phononic crystals capable of confining and guiding acoustic waves.[51] Notably, clever designs in periodic acoustic microstructures allow for fabricating the SAW equivalent of Dirac semimetals and insulators, which not only result in SAW topological protection but can also demonstrate the SAW analog of a quantum valley Hall system.[52] In a similar manner, acoustic periodic microstructures can mimic the physics of twisted 2D layered structures in an acoustic macroscopic platform.[53,54] Here, SAW transmission/absorption can act as a probe of the intriguing behavior of these acoustic analogs.[55]

Finally, we would like to mention that there are also interesting spin-related developments of SAWs coupling with nonmagnetic materials. In 2013, a theoretical study suggested that spin currents can be generated by the direct transfer of angular momentum from SAW induced lattice rotation to the electron spin in nonmagnetic materials, a mechanism known as spin-rotation coupling.[56] Although the first experimental realization of this spin-rotation coupling was claimed in a report in 2017,[57] the result is hindered by the presence of a magnetic layer coupled to SAWs. It would be desirable to find experimental evidence of the spin-rotation coupling in an all nonmagnetic structure and unleash its full potential. The challenge here is to detect the predicted low spin-conversion rf voltages due to spin-rotation coupling. One alternative is to characterize the spin accumulation by the high resolution magneto-optical Kerr effect (MOKE), as recently reported for charge induced spin accumulation in nonmagnetic systems.[58–60] Also recently, another study reported the generation of the spin current by the lattice motion induced by SAWs in nonmagnetic metallic layers with a strong spin–orbit interaction.[61] The spin current scales with the time derivative of the lattice displacement and is directly proportional to the amplitude of the spin Hall angle; however, it does not follow the expected spin Hall angle sign. The effect was termed

acoustic spin Hall effect and still awaits better understanding of its microscopic mechanism.

We have reviewed and provided our perspectives in a selected group of works involving spintronic devices with surface acoustic waves with particular emphasis on our own work and closely related reports. We would like to note that the large number of publications on this and similar topics forbids us to give justice to all, and most certainly, some relevant works escaped from our sight.

ACKNOWLEDGMENTS

We would like to express our gratitude to Kei Yamamoto and Mingran Xu for their valuable contributions to our SAW projects. We would also like to thank Thomas Lyons for proofreading our manuscript. Y.O. and J.P. are supported by Grants-in-Aid for Scientific Research (S) (No. 19H05629) and Japan Society for the Promotion of Science Grants-in-Aid for Scientific Research, translation from the original Japanese definition (No. 20H01865) from Ministry of Education, Culture, Sports, Science and Technology Japan. S.M. is supported by Japan Science and Technology Corporation Centers of Research Excellence in Science and Technology Grants (Nos. JPMJCR1954, JPMJCR1874, and JPMJCR20C1) and JSPS KAKENHI (Nos. 17H02927 and 20H01865) from MEXT Japan. Y.H. was supported by the RIKEN Junior Research Associate Program.

AUTHOR DECLARATIONS

Conflict of Interest

The authors have no conflicts to disclose.

DATA AVAILABILITY

The data that support the findings of this study are available from the corresponding author upon reasonable request.

REFERENCES

[1]J. P. Joule, Ann. Electr. Magn. Chem. **8**, 219–224 (1842).
[2]E. Villari, Rev. Phys. Chem **202**, 87 (1865).
[3]M. F. Lewis and E. Patterson, Appl. Phys. Lett. **20**, 276 (1972).
[4]W. Robbins and M. Lundstrom, Appl. Phys. Lett. **26**, 73 (1975).
[5]C. Kittel, Phys. Rev. **110**, 836 (1958).
[6]D. Afanasiev, I. Razdolski, K. Skibinsky, D. Bolotin, S. Yagupov, M. Strugatsky, A. Kirilyuk, T. Rasing, and A. Kimel, Phys. Rev. Lett. **112**, 147403 (2014).
[7]J. Janušonis, C. Chang, P. van Loosdrecht, and R. Tobey, Appl. Phys. Lett. **106**, 181601 (2015).
[8]N. I. Polzikova, S. G. Alekseev, V. A. Luzanov, and A. O. Raevskiy, J. Magn. Magn. Mater. **479**, 38–42 (2019).
[9]S. Alekseev, S. Dizhur, N. Polzikova, V. Luzanov, A. Raevskiy, A. Orlov, V. Kotov, and S. Nikitov, Appl. Phys. Lett. **117**, 072408 (2020).
[10]L. Dreher, M. Weiler, M. Pernpeintner, H. Huebl, R. Gross, M. Brandt, and S. Goennenwein, Phys. Rev. B **86**, 134415 (2012).
[11]K. Yamamoto, M. Xu, J. Puebla, Y. Otani, and S. Maekawa, J. Magn. Magn. Mater. **545**, 168672 (2022).
[12]P. Delsing, A. Cleland, M. Schuetz, J. Knörzer *et al.*, J. Phys. D: Appl. Phys. **52**, 353001 (2019).
[13]S. Davis, A. Baruth, and S. Adenwalla, Appl. Phys. Lett. **97**, 232507 (2010).
[14]A. Biswas, S. Bandyopadhyay, and J. Atulasimha, Appl. Phys. Lett. **103**, 232401 (2013).
[15]J. Puebla, J. Kim, K. Kondou, and Y. Otani, Comm. Mater. **1**, 24 (2020).
[16]J. Dean, M. Bryan, J. Cooper, A. Virbule, J. E. Cunningham, and T. Hayward, Appl. Phys. Lett. **107**, 142405 (2015).
[17]W. Edrington, U. Singh, M. Dominguez, J. Alexander, R. Nepal, and S. Adenwalla, Appl. Phys. Lett. **112**, 052402 (2018).
[18]A. Adhikari, E. Gilroy, T. Hayward, and S. Adenwalla, J. Phys.: Condens. Matter **33**, 31LT01 (2021).
[19]L. Thevenard, I. S. Camara, J.-Y. Prieur, P. Rovillain, A. Lemaıtre, C. Gourdon, and J.-Y. Duquesne, Phys. Rev. B **93**, 140405 (2016).
[20]T. Yokouchi, S. Sugimoto, B. Rana, S. Seki, N. Ogawa, S. Kasai, and Y. Otani, Nat. Nanotechnol. **15**, 361–366 (2020).
[21]M. Weiler, L. Dreher, C. Heeg, H. Huebl, R. Gross, M. Brandt, and S. Goennenwein, Phys. Rev. Lett. **106**, 117601 (2011).
[22]Y. Tserkovnyak, A. Brataas, and G. Bauer, Phys. Rev. B **66**, 224403 (2002).
[23]M. Weiler, H. Huebl, F. Goerg, F. Czeschka, R. Gross, and S. Goennenwein, Phys. Rev. Lett. **108**, 176601 (2012).
[24]J. Puebla, M. Xu, B. Rana, K. Yamamoto, S. Maekawa, and Y. Otani, J. Phys. D: Appl. Phys. **53**, 264002 (2020).
[25]M. Xu, J. Puebla, F. Auvray, B. Rana, K. Kondou, and Y. Otani, Phys. Rev. B **97**, 180301 (2018).
[26]Y. Hwang, J. Puebla, M. Xu, A. Lagarrigue, K. Kondou, and Y. Otani, Appl. Phys. Lett. **116**, 252404 (2020).
[27]R. Sasaki, Y. Nii, Y. Iguchi, and Y. Onose, Phys. Rev. B **95**, 020407 (2017).
[28]A. Hernández-Mínguez, F. Macià, J. Hernńndez, J. Herfort, and P. Santos, Phys. Rev. Appl. **13**, 044018 (2020).
[29]R. Verba, I. Lisenkov, I. Krivorotov, V. Tiberkevich, and A. Slavin, Phys. Rev. Applied **9**, 064014 (2018).
[30]M. Küß, M. Heigl, L. Flacke, A. Hörner, M. Weiler, M. Albrecht, and A. Wixforth, Phys. Rev. Lett. **125**, 217203 (2020).
[31]P. Shah, D. Bas, I. Lisenkov, A. Matyushov, N. Sun, and M. Page, Sci. Adv. **6**, eabc5648 (2020).
[32]M. Küß, M. Heigl, L. Flacke, A. Hörner, M. Weiler, A. Wixforth, and M. Albrecht, Phys. Rev. Appl. **15**, 034060 (2021).
[33]R. Verba, V. Tiberkevich, and A. Slavin, Phys. Rev. Appl. **12**, 054061 (2019).
[34]R. Sasaki, Y. Nii, and Y. Onose, Nat. Commun. **12**, 2599 (2021).
[35]S. Maekawa and M. Tachiki, AIP Conf. Proc. **29**, 542 (1976).
[36]M. Xu, K. Yamamoto, J. Puebla, K. Baumgaertl, B. Rana, K. Miura, H. Takahashi, D. Grundler, S. Maekawa, and Y. Otani, Sci. Adv. **6**, eabb1724 (2020).
[37]S. Tateno and Y. Nozaki, Phys. Rev. Appl. **13**, 034074 (2020).
[38]L. Thevenard, C. Gourdon, J. Y. Prieur, H. J. von Bardeleben, S. Vincent, L. Becerra, L. Largeau, and J.-Y. Duquesne, Phys. Rev. B **90**, 094401 (2014).
[39]J. Shi, D. Ahmed, X. Mao, S.-C. Lin, A. Lawita, and T. Huang, Lab Chip **9**, 2890 (2009).
[40]H. Ge, X.-Y. Xu, L. Liu, R. Xu, Z.-K. Lin, S.-Y. Yu, M. Bao, J.-H. Jiang, M.-H. Lu, and Y.-F. Chen, Phys. Rev. Lett. **127**, 144502 (2021).
[41]D. K. S. Haroche, Phys. Today **42**(1), 24 (1989).
[42]J. Puebla, Y. Hwang, K. Kondou, and Y. Otani, Ann. Phys. **534**(4), 2100398 (2022).
[43]D. Bozhko, P. Clausen, G. Melkov, V. L'vov, A. Pomyalov, V. Vasyuchka, A. Chumak, B. Hillebrands, and A. Serga, Phys. Rev. Lett. **118**, 237201 (2017).
[44]K. Bliokh and F. Nori, Phys. Rev. B **99**, 174310 (2019).
[45]Z. Tian, Z. Wang, P. Zhang, T. Naquin, J. Mai, Y. Wu, S. Yang, Y. Gu, H. Bachman, Y. Liang, Z. Yu, and T. Huang, Sci. Adv. **6**, eabb0494 (2020).
[46]I. Toftul, K. Bliokh, and M. Petrov, AIP Conf. Proc. **2300**, 020127 (2020).
[47]H. Zhuang, P. Kent, and R. Hennig, Phys. Rev. B **93**, 134407 (2016).
[48]S. Jiang, H. Xie, J. Shan, and K. Mak, Nat. Mater. **19**, 1295 (2020).
[49]D. K. D. MacNeill, J. T. Hou, P. Zhang, P. Jarillo-Herrero, and L. Liu, Phys. Rev. Lett. **123**, 047204 (2019).
[50]L. Brillouin, *Wave Propagation in Periodic Structures* (Dover Publications, 1946).
[51]M. Assouar and M. Oudich, Appl. Phys. Lett. **99**, 123505 (2011).
[52]J.-Q. Wang, Z.-D. Zhang, S.-Y. Yu, H. Ge, K.-F. Liu, T. Wu, X.-C. Sun, L. Liu, H.-Y. Chen, C. He, M.-H. Lu, and Y.-F. Chen, Nat. Commun. **13**, 1324 (2022).
[53]Y. Deng, M. Oudich, N. J. Gerard, J. Ji, M. Lu, and Y. Jing, Phys. Rev. B **102**, 180304 (2020).

[54]S. Gardezi, H. Pirie, S. Carr, W. Dorrell, and J. Hoffman, 2D Mater. **8**, 031002 (2021).
[55]S.-Y. Yu, X.-C. Sun, X. Ni, Q. Wang, X.-J. Yan, C. He, X.-P. Liu, L. Feng, M.-H. Lu, and Y.-F. Chen, Nat. Mater. **15**, 1243 (2016).
[56]M. Matsuo, J. Ieda, K. Harii, E. Saitoh, and S. Maekawa, Phys. Rev. B **87**, 180402 (2013).
[57]D. Kobayashi, T. Yoshikawa, M. Matsuo, R. Iguchi, S. Maekawa, E. Saitoh, and Y. Nozaki, Phys. Rev. Lett. **119**, 077202 (2017).
[58]J. Puebla, F. Auvray, M. Xu, B. Rana, A. Albouy, H. Tsai, K. Kondou, G. Tatara, and Y. Otani, Appl. Phys. Lett. **111**, 092402 (2017).
[59]C. Stamm, C. Murer, M. Berritta, J. Feng, M. Gabureac, P. Oppeneer, and P. Gambardella, Phys. Rev. Lett. **119**, 087203 (2017).
[60]F. Auvray, J. Puebla, M. Xu, B. Rana, D. Hashizume, and Y. Otani, J. Mater. Sci. **29**, 15664 (2018).
[61]T. Kawada, M. Kawaguchi, T. Funato, H. Kohno, and M. Hayashi, Sci. Adv. **7**, eabd9697 (2021).